

## CALCULATION OF BENDING MOMENTS UNLOADING FEMUR AND TIBIA BONES

Munih, M., Kralj, A., Bajd, T.

Faculty of Electrical and Computer Engineering, Edvard Kardelj University  
Ljubljana, YUGOSLAVIA

### ABSTRACT

The results presented are through biomechanical measurements and modelling supporting the Pauwels hypothesis that skeletal muscles are not only producing joint moments, providing posture and movement, but also reducing the bending torques caused by external loads along the long bones. Lower limbs of eleven normal subjects in two different standing postures were taken into consideration.

KEY WORDS: bending moment, biomechanical modelling, musculo-skeletal system

### INTRODUCTION

Only few researchers in the past studied the close collaboration of bone and skeletal muscle. Galileo Galilei (1638, Baron 1983) was first who related the bone shape to its function, while more profound studies on bone stressing were published by Koch (1917) in his book *The Laws of Bone Architecture*. Very detailed and a reaching relations were first clearly expressed and explained by Pauwels (1980). His theoretical studies, published in the book *Biomechanics of Locomotor Apparatus*, have led to the hypothesis that the bending torque loading of long bones, for instance in lower extremity, is invariant with respect to posture selected or movement performed because of active muscle reduction of stressing. The basic idea of bone unloading, initiated by his work, is illustrated in Figure 1. In Figure 1c the bending moment theoretically equals zero, while the compression stressing is increased. This results in significant bone material saving. The same law applies for more complicated bone shapes and also for synergistic muscle activation.

This paper discusses for the first time the in-vivo testing of the stated principles through biomechanical measurements and calculations of bending moments for femur and tibia bones in the sagittal plane including nineteen lower extremity muscles. Numerical data were assessed in two static standing postures: normal upright standing and standing while leaned forward in eleven healthy male persons, while only three are presented here. This presentation highlights the calculated bending moments with only brief model and measurement description. The results obtained are improving our

understanding and knowledge of basic functioning and biomechanical principles governing musculo-skeletal system. Such new criteria is important for artificial muscle activation such as functional electrical stimulation as it was proposed by Kralj and Bajd (1989).

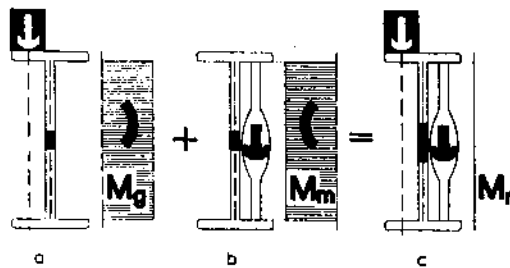


Figure 1 Bending moment caused by external load (a) is effectively compensated (c) by muscle force (b)

## METHODOLOGY

For the bending moment calculation along the lower extremity bones, the existing biped models cannot be directly implemented. Most mathematical models of lower extremities are dealing with the dynamic properties relevant for description of gait (Chow and Jacobson, 1971; Hatze, 1976; Khang&Zajac, 1989). The models usually include gravitational and inertial forces or torques together with centrifugal and Coriolis contributions and ligament moments. In some of these models the muscles action is taken into account (Hatze, 1977; Khang et al, 1989). The muscle is usually described as consisting of an active contractile element as first proposed by Hill (1949). In contrary several authors (Seireg and Arkivar, 1973, 1975; Crowninshield, 1978; Hardt, 1978; Dul et al, 1984) calculate muscle forces through different optimization procedures. They use different types of linear or nonlinear optimization functions. Our model, which is also assisted by the techniques mentioned, will be described in four steps: anatomical and laboratory measurements of the data required, muscle force optimization and bending moment calculation.

## Anatomical Measurements

When studying the bending moments and possible bone damages anatomical musculo-skeletal model of the lower extremity should be developed for muscle force and moment calculation. It must include:

- exact shapes, positions and orientations of muscle attachments,
- exact shapes of bones,
- the points of the resultant muscle activity,
- directions of the muscle force vectors.

Because of lack of accurate anthropometrical numerical data for several muscle attachments and bones of lower extremity in the existing literature, there was necessary to measure the data required.

The muscles were first carefully, along the natural layers and planes, one by one dissected from the specimen. The attachment points were marked by pins up to 10 mm apart. Their x, y, z coordinates were measured and entered into computer. There were found three types of shapes for muscle attachments (see Figure 2):

- very small areas with the diameter of only few millimetres,
- large attachment areas,
- attachment curves.

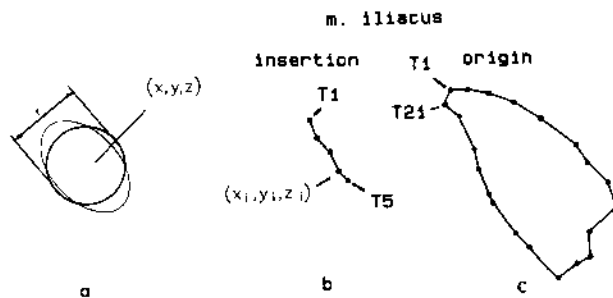


Figure 2 Muscle attachments as measured and represented in the computer

no.	Muscle	VOLUME (ml)	TENDON (mm)	CROSS-SEC (mm)	Fmax(N) 30 N/cm <sup>2</sup>	fmax(N) 50 N/cm <sup>2</sup>	abbreviations
1.	m. sartorius	125	75	240	72	120	sar
2.	m. gracilis	80	100	270	81	135	gr
3.	m. semitendinosus	170	150	660	198	330	sat
4.	m. gluteus max.	620	/	4944	1483.2	2472	gma
5.	m. tensor fasciae latae	75	385	330	99	165	tft
6.	m. biceps f. cap. longum	220	36	630	189	315	bfl
	m. biceps f. cap. brevius	?	36	300	90	150	bfb
7.	m. gluteus medius	280	/	2170	651	1085	gml, gml
8.	m. adductor magnus	320	80	1540	462	770	am, amf
9.	m. quadriceps femoris	1650	/	4340	1302	2170	
	rectus femoris	/	/	720	216	360	rtz, rfs
	vastus lateralis	/	/	930	279	465	vl
	vastus medialis+intermedius	/	/	1750	525	875	vm, vl
10.	m. iliacus	200	/	770	231	385	il
11.	m. psoas major	?	/	930	279	465	pm
12.	m. adductor longus	130	15	760	228	380	al
13.	m. semimembranosus	170	102	750	225	375	sam
14.	m. gastrocnemius	420	145	1190	357	595	gast, gasm
15.	m. soleus		50	1470	441	735	sol, sole
16.	m. tibialis anterior	110	104	540	162	270	ta
17.	m. peroneus longus	60	212	220	66	110	pl
18.	m. peroneus brevis	40	60	120	36	60	pb
19.	m. flexor digitorum longus	70	#	240	72	120	dl

Table 1 Volume, tendon length, cross-section and estimated maximal force of dissected lower limb muscles

In the first case only the center of the attachment was assessed together with the corresponding diameter. In the second case several coordinates were measured along the circumference of the attachment area. In the similar way the coordinates were assessed also along the attachment curves. Most of the muscles have the latter type of the attachment while very small attachment areas are not very frequent. Several attachments (*m. gluteus medius*, *m. adductor magnus*, *m. rectus femoris*, *m. gastrocnemius* and *soleus*) consist of combined attachments or have two muscle insertions or origins. These are the reasons to divide and consider those muscles as two muscles.

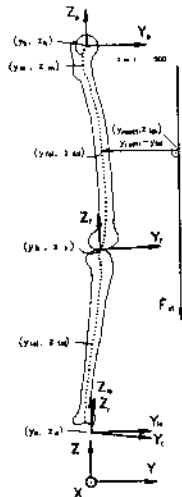


Figure 3 Bone central line points, markers and coordinate systems

For each muscle separated from the specimen also the following characteristic parameters were determined (Table 1): maximal cross-section area, muscle volume and tendon length. The next task is to find geometrical shapes of the lower limb bones, femur and tibia. To assure the same accuracy of the measurements and because of simplicity, the necessary numerical data were gathered in the same way and by the same instrumentation as the data describing the muscle attachments. The model was built in the sagittal plane, so that the anterior part of the femur was represented by 20 points, while the posterior part by 28. Similarly, the shape of the tibia was modelled with 20 points in the posterior part and 17 points in the anterior part. Anterior and posterior points were interpolated (Natural Cubic Spline) at the same height  $z$ . In this way the points on the bone central line (Figure 3) were calculated. These points are very important, because all the bending moments were determined through the levers determined according to this central line.

The fibula bone has not been included into the present model. The calculation of the distribution of the muscle forces between the tibia and fibula would extremely complicate already complex mathematical model. Skeletal muscles, having attachments on the fibula, were treated as belonging to the tibia. The determination of the bone shape around the hip, knee and ankle joints was improved by increasing the number of points by reading them from the X-ray photograph. X-ray photography alone did not yield sufficiently accurate data because of nonlinearities of the photographing system.

From the data gathered, it is possible to determine the directions of the muscle force activity. In general two approaches are possible:

- the straight line model,
- the centroid model.

In the first case the straight line is passing between two muscle attachments (Dostal and Andrews, 1981; Brand et al, 1982). The centroid line model requires that the positions of the transverse cross-sectional centroids are established for each

muscle. The muscle force is represented by a tangent to the centroid line at the observed point. The complexity of the lower limb model, including 19 muscles, would increase considerably by taking into account the centroid model. The centroid line model obtained from cadaver may not accurately represent the real situation. In addition to the disadvantages mentioned, it was found by Jensen and Davy (1975) that the differences between these two approaches were estimated to vary from 1 to 12 percents. The straight line model was therefore chosen in the present study.

### Laboratory Measurements

Besides anatomical data also the measurements of standing postures are necessary. The following parameters were measured in all healthy male subjects:

- *anthropometric parameters,*
- *positions of characteristic body points in sagittal and coronal planes,*
- *ground reaction forces and moments.*

Average age of subjects was 29 years (23 - 43), average height 174 cm (152 - 185) and average body weight 66.9 kg (48.3 - 77.5).

Exact anthropometric lengths and body postures were assessed by the help of four markers attached to the right body side to capture the body posture in sagittal plane. Distances between all the markers (Figure 3): ankle/knee, knee/hip, hip/shoulder and ankle/force plate (FP), were measured with  $\pm 0.5$  mm accuracy. Marker coordinates were assessed through black and white photography in sagittal plane. The coordinates were entered into computer via film projection on to the graphic tablet. Seven points were recorded in each frame. Except the four points mentioned, two additional points of the plumb line were recorded. The plumb line was placed for exact vertical position assessment. From the data obtained, ankle, knee and hip angles were calculated.

The position and magnitude of the ground reaction force is needed in our model in order to calculate the bending moments along the long bones of the lower extremities. The AMTI (Advanced Mechanical Technology OR6-5-1) force plate (FP) with strain gauge transducers was used. The person measured was asked to place the right leg on FP, and the left leg on a wooden support which had the same size as FP. The angle between the left and right feet was always  $30^{\circ}$  both feet were placed with heels together in such a way that the anterior/posterior  $y^a$  coordinate was aligned with the FP to be zero. Before the measurement all the markers were placed and the anthropometric data measured. The subject was asked to remain in the same posture for one minute. In that time the force plate parameters were collected by the computer and pictures were taken after 20s and 40s time. The selected postures were: standing leaned forward and normal standing posture.

Anatomical data assessed in cadaver were transformed regarding the data measured during standing posture of subjects. The described numerical data of femur and tibia center line together with muscle origin and insertion were called from library when bending moments calculation was started. Following scaling procedure, rotation around different centers of joint rotation and coordinates translation into the reference coordinate system was performed. The moments were calculated in world (global) coordinate system.

The model presented is also incorporating different segment density values. Each limb segment has different combination of bone, muscles, fat and other tissue components. More distal segments have greater density. This consideration should be included into the  $F_z$  force. According to Winter (1979) feet  $d_f$  shank  $d_s$  and thigh  $d_t$  densities as function of total body height and weight were determined.

### Gravitational Bending Moment Calculation

Our next goal was to determine the bending moments along the long bones: femur and tibia. The resultant bending moment acting on the bone is actually a sum of:

- bending moment caused by gravitational force,
- bending moments caused by muscle force activity.

The bending moments are calculated along the bone center line (Figure 3). The femur or tibia center line is composed from five hundred equidistant points  $z_{fc_i}$  in vertical direction (Figure 3)(index  $f$  is used for femur and  $t$  for tibia,  $i = 1 \dots 500$ ). The point  $z_{fc_1}$  is the highest and  $z_{fc_{500}}$  the lowest. The distance between two neighbour points is less than 1mm.  $F_z$  force, representing half of the body weight, was determined as an average over one second of the whole sampling. The gravitational force  $F_{z1}$  in the hip results from the trunk, arms and head weight, without thigh  $m_t$ , shank  $m_s$  and feet  $m_f$  contribution:

$$F_{z1} = F_z - (m_t + m_s + m_f)g, \quad g = 9,81 \text{ m/s}^2 \quad (1)$$

$F_{z2}$  in the knee equals:

$$F_{z2} = F_{z1} + m_t g \quad (2)$$

From FP average values of ground reaction force application  $y_c$  and moment  $M_x$  can be determined. By the help of Winter's (1979) data, mass centers for feet  $y_{fo}$ , shank  $y_{so}$  and thigh  $y_{to}$  can be calculated in reference coordinates.

$$y_{fo} = 0,0262 l_f \quad (3)$$

$$y_{so} = (1-0,433)y_k \quad (4)$$

$$y_{to} = y_t + 0,433 l_t \quad (5)$$

This is necessary in order to determine the coordinate of the force  $F_{z1}$  acting at the hip level:

$$y_{rest1} = \frac{M_x - (y_{fo} m_f + y_{so} m_s + y_{to} m_t)}{m_f + m_s + m_t} \quad (6)$$

Similarly  $y_{rest2}$  can be found for the force  $F_{z2}$  acting at the knee level:

## CONCLUSIONS AND DISCUSSION

The plausibility of the hypothesis that short, supramaximal stimulation of quadriceps during the cyclical lower leg movement results in minimal torque-time integral for a given angle range was illustrated in simulations. The remaining question is whether minimal torque-time integral corresponds to minimal muscle activation in short bursts of stimulation at constant stimulation frequency. This is determined by the muscle dynamics: the torque generated by the muscle takes some time to reach a maximum, and also depends on muscle length and muscle shortening or lengthening velocity.

The discrete time PID controller appeared to be able to realize the reference angle  $\varphi_{max\ ref}$ , and compensate the influence of fatigue by adapting the stimulation burst time  $T_{on}$ . The time periods of the experiments should be taken longer than 150 s when fatigue compensation is to be investigated more extensively. In principle, this method for adapting open loop stimulation patterns on the basis of the performance in previous cycles is possible for a complete walking movement as well. However, it will be more difficult to design rules for the adaptation of the stimulation patterns of the individual muscles on the basis of measurements of the total coordinated walking movement, because the movement is very complex, and the muscle actions interact. Furthermore, changing external circumstances during walking requires a fast response of the controller.

## REFERENCES

- 1 D.R. McNeal, R.J. Nakai, P. Meadows and W. Tu, "Open-Loop Control of the Freely-Swinging Paralyzed Leg", IEEE Trans.Biomed.Eng., Vol. 36, 1989, pp. 895-905.
- 2 E.B. Marsolais and R. Kobetic, Functional Walking in Paralyzed Patients by Means of Electrical Stimulation, Clinical Orthopaedics, Vol. 175, 1983, pp. 30-36.
- 3 H.J. Chizeck, R. Kobetic, E.B. Marsolais, J.J. Abbas, I.H. Donner and E. Simon, Control of Functional Neuromuscular Stimulation Systems for Standing and Locomotion in Paraplegics, Proc. IEEE, Vol. 76, 1988, pp. 1155-1165.

## CONCLUSIONS AND DISCUSSION

The plausibility of the hypothesis that short, supramaximal stimulation of quadriceps during the cyclical lower leg movement results in minimal torque-time integral for a given angle range was illustrated in simulations. The remaining question is whether minimal torque-time integral corresponds to minimal muscle activation in short bursts of stimulation at constant stimulation frequency. This is determined by the muscle dynamics: the torque generated by the muscle takes some time to reach a maximum, and also depends on muscle length and muscle shortening or lengthening velocity.

The discrete time PID controller appeared to be able to realize the reference angle  $\varphi_{max\ ref}$ , and compensate the influence of fatigue by adapting the stimulation burst time  $T_{on}$ . The time periods of the experiments should be taken longer than 150 s when fatigue compensation is to be investigated more extensively. In principle, this method for adapting open loop stimulation patterns on the basis of the performance in previous cycles is possible for a complete walking movement as well. However, it will be more difficult to design rules for the adaptation of the stimulation patterns of the individual muscles on the basis of measurements of the total coordinated walking movement, because the movement is very complex, and the muscle actions interact. Furthermore, changing external circumstances during walking requires a fast response of the controller.

## REFERENCES

- 1 D.R. McNeal, R.J. Nakai, P. Meadows and W. Tu, "Open-Loop Control of the Freely-Swinging Paralyzed Leg", IEEE Trans. Biomed. Eng., Vol. 36, 1989, pp. 895-905.
- 2 E.B. Marsolais and R. Kobetic, Functional Walking in Paralyzed Patients by Means of Electrical Stimulation, Clinical Orthopaedics, Vol. 175, 1983, pp. 30-36.
- 3 H.J. Chizeck, R. Kobetic, E.B. Marsolais, J.J. Abbas, I.H. Donner and E. Simon, Control of Functional Neuromuscular Stimulation Systems for Standing and Locomotion in Paraplegics, Proc. IEEE, Vol. 76, 1988, pp. 1155-1165.